



Influence of heat losses on nonlinear fingering dynamics of exothermic autocatalytic fronts

J. D'Heroncourt, A. De Wit*

Nonlinear Physical Chemistry Unit, Service de Chimie Physique et Biologie Théorique, Faculté des Sciences, Université Libre de Bruxelles (ULB), CP 231, Campus Plaine, 1050 Brussels, Belgium

ARTICLE INFO

Article history:

Available online 16 July 2009

Communicated by J. Lega

Keywords:

Fingering
Autocatalytic fronts
Convection
Rayleigh–Taylor
Buoyancy

ABSTRACT

Across traveling exothermic autocatalytic fronts, a density jump can be observed due to changes in composition and temperature. These density changes are prone to induce buoyancy-driven convection around the front when the propagation takes place in absence of gel within the gravity field. Most recent experiments devoted to studying such reaction-diffusion-convection dynamics are performed in Hele–Shaw cells, two glass plates separated by a thin gap width and filled by the chemical solutions. We investigate here the influence of heat losses through the walls of such cells on the nonlinear fingering dynamics of exothermic autocatalytic fronts propagating in vertical Hele–Shaw cells. We show that these heat losses increase tip splittings and modify the properties of the flow field. A comparison of the differences between the dynamics in reactors with respectively insulating and conducting walls is performed as a function of the Lewis number Le , the Newton cooling coefficient α quantifying the amplitude of heat losses and the width of the system. We find that tip splitting is enhanced for intermediate values of α while coarsening towards one single finger dominates for insulated systems or large values of α leading to situations equivalent to isothermal ones.

© 2009 Elsevier B.V. All rights reserved.

The coupling between autocatalytic chemical reactions and diffusion can lead to traveling fronts whereby products invade fresh reactants at a constant speed. The properties of these fronts have been studied in details in gels used to avoid any convective motions. In absence of gels, the dynamics can be perturbed by convective currents due either to buoyancy or Marangoni effects. In this context, S.C. Müller has largely contributed to characterize spatio-temporal dynamics due to convective motions deforming waves traveling in shallow layers open to the air or closed reactors [1–12]. In the case of the iodate–arsenous acid (IAA) reaction traveling in vertical Hele–Shaw cells, Müller and Böckmann have for the first time measured experimentally dispersion curves giving the growth rate of the perturbations as a function of their wavenumber at early times in the dynamics [10]. In such reactors, a Rayleigh–Taylor instability occurs when the IAA front travels upwards in the gravity field as the reactants are slightly heavier than the products. They have moreover characterized experimentally the dynamics in the long time nonlinear regime [11] showing that, after a general coarsening trend, tip splittings can occur for large cells. More recently, we have shown in collaboration that heat effects due to the exothermicity of the reaction can affect the dynamics leading, for conducting walls,

to a velocity field organized as a quadrupole instead of a dipole obtained in insulated systems [12].

To gain more insight into the influence of such thermal effects in buoyancy-driven convection around fronts, let us recall that, across an autocatalytic front, the density variation $\Delta\rho = \rho_p - \rho_r$ (i.e. the difference between the density of the product ρ_p and that of the reactant ρ_r) is the sum of a solutal $\Delta\rho_c$ and a thermal $\Delta\rho_T$ part [13–16]. As no endothermic autocatalytic reaction is known, the density decreases typically during an exothermic reaction due to the thermal effects i.e. $\Delta\rho_T < 0$. The solutal component on the other hand can have both a positive or negative sign depending whether the composition change decreases ($\Delta\rho_c < 0$ like in the IAA reaction) or increases the density ($\Delta\rho_c > 0$ like in the chlorite–tetrathionate - CT - reaction for instance [17,18]).

Solutal and thermal contributions to the density jump across the front can thus either be opposite or reinforce each other [16]. In isolated systems where no heat is lost to the surroundings and when $\Delta\rho_c$ and $\Delta\rho_T$ have the same sign, simple Rayleigh–Taylor convection is observed for ascending fronts featuring heavy reactants at room temperature above hotter and solute lighter products [10,11,19–22] while in specific cases, differential diffusive effects can destabilize descending fronts [23]. When the two contributions are opposite they lead to multicomponent convection and double diffusive instabilities [14–16,24,25]. Fingering in such competitive situations has been studied in the CT reaction both experimentally [18,26–28] and theoretically [15,26] showing

* Corresponding author.

E-mail address: adewit@ulb.ac.be (A. De Wit).

that a sufficiently strong exothermicity can destabilize otherwise stable front and lead to new dynamics.

Experimental evidences [12,26,29–33] and theoretical work [12,31,33,34] have however shown that heat losses through the walls of the reactor can have an important influence on the dynamics. When thermal effects cannot be neglected (i.e. for more exothermic reactions or thicker cells [33]), stability properties and nonlinear dynamics can be affected. In capillary tubes, it has already been shown long ago that changing the surrounding medium around the tube can modify the stability properties of the front [19,29] while measurements of the heat variation during an experiment in a tube yields a thermal change smaller than in adiabatic conditions pointing out to the existence of heat losses [30]. Furthermore a change in the material of the walls of the Hele–Shaw cell have also proved to change the stability of the fronts [26]. From a theoretical point of view, it has been shown that, in the cooperative case, thermal leaks can change the fingering dynamics [12,34] in the sense that stable downward propagating cooperative fronts can become unstable due to the change of the temperature profile from a front to a localized pulse solution. On the other hand, upward propagating fronts can for some values of parameters feature more frequent tip splitting. Furthermore the flow field is shown to change from a two convection roll situation in the absence of heat losses to a four vortices one in their presence [12]. In antagonistic reactions like the CT system, hot spots have been observed experimentally for conducting walls [32]. A detailed understanding of the role of heat losses on the nonlinear dynamics as a function of the various values of the parameters of the problem is however still missing.

In this context, it is the objective of this article to provide an extensive numerical analysis of the influence of heat losses through the walls of the reactor in the nonlinear fingering dynamics of cooperative exothermic reactions for which the solutal and thermal part to the density jump across the front have the same sign. For cooperative fronts, density effects lead in insulated systems to typically buoyantly unstable upward propagating fronts as they correspond to a stratification of heavy reactants at room temperature on top of lighter and hotter products. The nonlinear evolution of fingers is then the same as that for isothermal systems with $\Delta\rho_s < 0$ as has been studied with the IAA reaction both experimentally [11] and theoretically [22]. These studies show that, after an initial linear regime where the properties of fingers is well described by dispersion curves [10,35,36] and a well defined wavelength [37], fingers start to merge and coarsen towards larger fingers [11,21,22]. In narrow systems, the asymptotic dynamics is one single finger of constant length and speed [19–21] featuring self-similar properties [22,38]. In larger systems or for larger Rayleigh numbers, fingers undergo tip splittings events whereby a sufficiently large finger breaks into two smaller fingers [11,12,22]. Similar observations of coarsening towards one single finger in narrow systems and occurrence of tip splitting in larger ones have also been obtained for the CT reaction when thermal effects can be neglected [39,40]. In order to understand how heat losses through the walls can affect these properties for exothermic reactions, we perform here a detailed parametric study of the influence of heat losses through a Newton coefficient α , of the Lewis number and of the width of the cell on the nonlinear fingering dynamics of exothermic cooperative fronts. We show that heat losses favor tip splitting events which remain present even when heat diffusion is quite large. While single fingers can be obtained either for insulated systems or large heat losses, tip splitting is encountered for intermediate values of α . We moreover study the change in the properties of convection rolls as a function of the heat loss intensity α .

The paper is organized as follows. In Section 2 we present the model and the numerical method used to integrate the nonlinear evolution equations. In Section 3 we perform a parametric study before characterizing the flow field in Section 4. We then briefly conclude in Section 5.

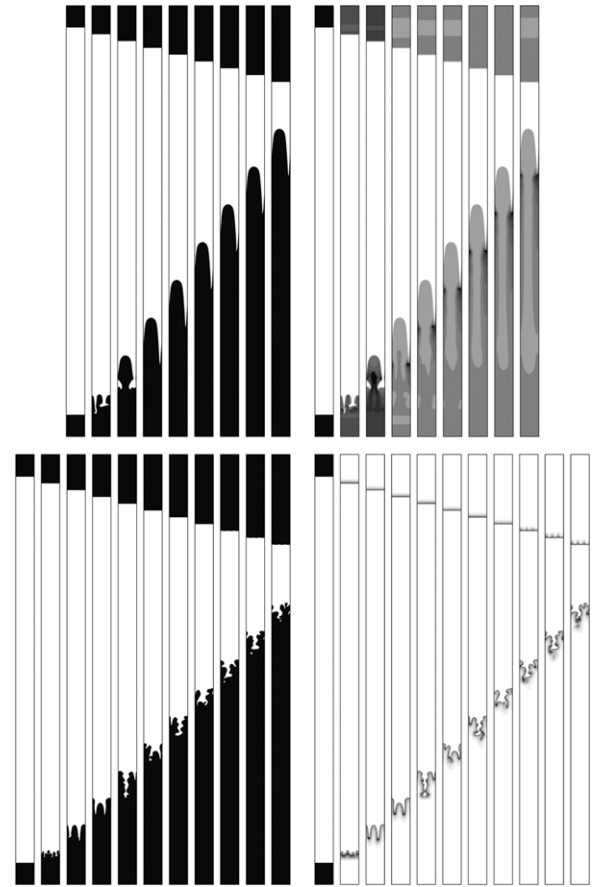


Fig. 1. Nonlinear dynamics of concentration (left) and temperature (right) in the fingering of exothermic reaction-diffusion fronts respectively without (top) and with (bottom) heat losses for the parameters $Le = 5$, $Da = 0.3$, $\gamma_T = -5$. The time interval between two images is 500 units of time. The width of the integration domain is $L_y = 512$. For the isolated case ($\alpha = 0$, top) the descending front is stable while the ascending one features coarsening towards one single finger traveling with constant shape and speed. For the conducting case ($\alpha = 0.01$, bottom) the descending front is unstable as witnessed by the small undulation of the interface visible in the T field. The ascending front features tip splittings.

1. Model

The model system is a Hele–Shaw cell of length L_x oriented along the gravity field and of width L_y . This cell has a gapwidth $h \ll L_x, L_y$, sufficiently thin to consider the incompressible velocity field $\underline{u} = (u_x, u_y)$ as two dimensional and evolving following Darcy's law (1) coupled to reaction-diffusion-convection equations for the concentration c of the autocatalytic product (4) and temperature T (5) through the dimensionless model [15,34]:

$$\nabla p = -\underline{u} + \rho(c, T)\underline{i}_x, \quad (1)$$

$$\rho = (1 - c) + \gamma_T T, \quad (2)$$

$$\nabla \cdot \underline{u} = 0, \quad (3)$$

$$\frac{\partial c}{\partial t} + \underline{u} \cdot \nabla c = \nabla^2 c - Da c(c - 1)(c + d), \quad (4)$$

$$\frac{\partial T}{\partial t} + \underline{u} \cdot \nabla T = Le \nabla^2 T - Da c(c - 1)(c + d) - \alpha T. \quad (5)$$

In Darcy's law, the density depends on c and T as (2) where $\gamma_T < 0$ is the dimensionless thermal expansion coefficient quantifying the thermal contribution to the density jump across the front [12,15,34]. In practice, it measures the ratio between the thermal density change $\Delta\rho_T$ relative to the solutal one $\Delta\rho_c$ and it is therefore a negative quantity as $\Delta\rho_T < 0$ while $\Delta\rho_c > 0$ in the

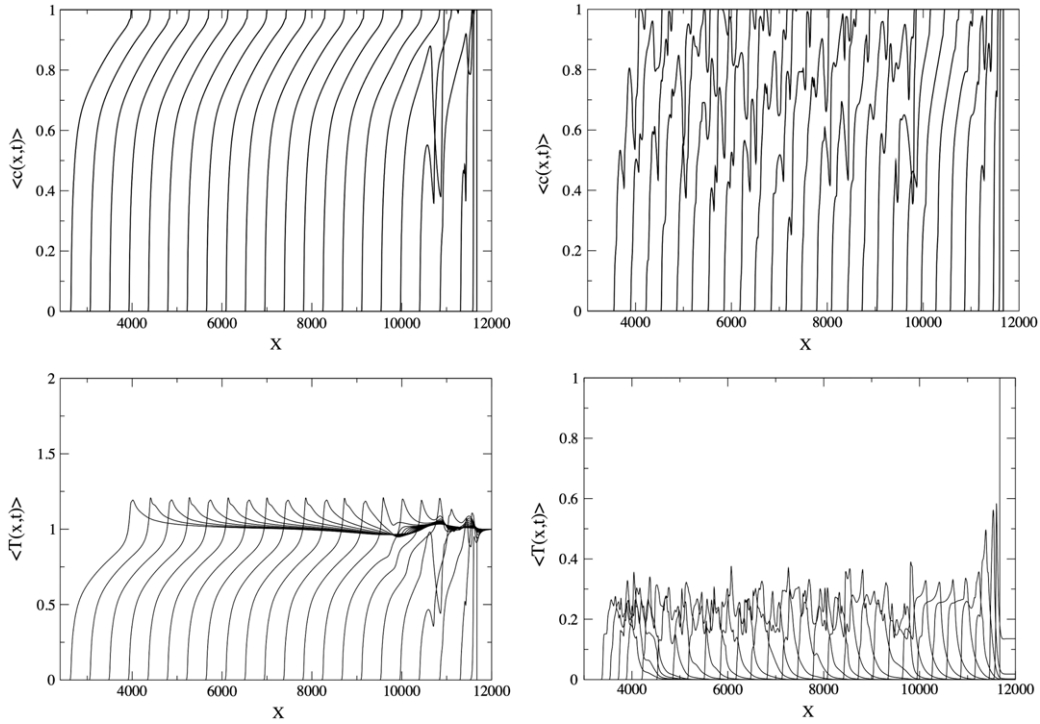


Fig. 2. Transversely averaged profiles of the concentration c (top) and temperature T (bottom) for the upward moving front (i.e. moving here towards decreasing values of x) in the case of insulating walls ($\alpha = 0$, left column) or conducting walls ($\alpha = 0.01$, right column) for the simulations of Fig. 1. The time interval between two successive curves is $\Delta t = 200$.

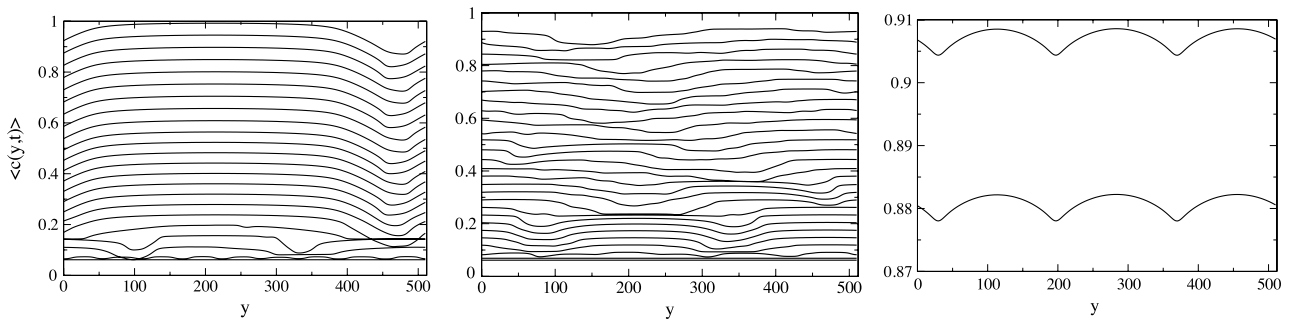


Fig. 3. Longitudinally averaged profiles of concentration for the simulations of Fig. 1 in the case of insulating walls i.e. $\alpha = 0$ on the left, and with conducting walls i.e. $\alpha = 0.01$ in the center for the upward propagating front. The right figure shows the averaged profile for the unstable downward propagating front when $\alpha = 0.01$. The time interval between two successive curves is $\Delta t = 200$.

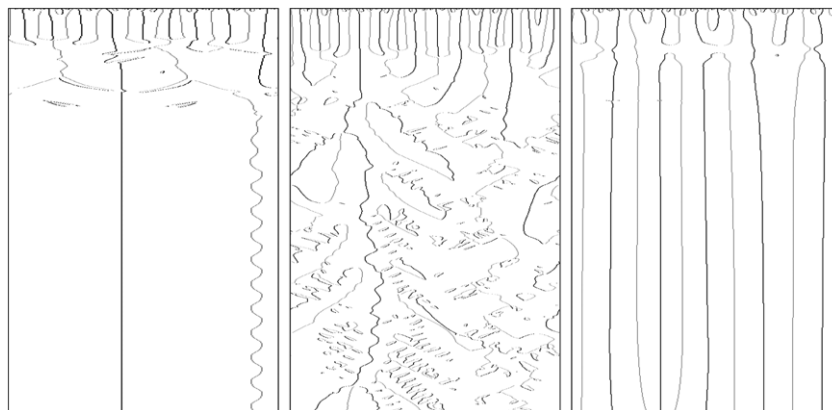


Fig. 4. Space-time maps of the locations of the maxima (black) and minima (grey) of the transversely averaged profiles $\langle c(y,t) \rangle$ for the simulations of Fig. 1 for the cases of the ascending front when $\alpha = 0$, and the upward and downward moving fronts when $\alpha = 0.01$ from left to right respectively. The horizontal direction corresponds to the y direction ($L_y = 512$) while time is increasing downwards up to $t = 4400$.

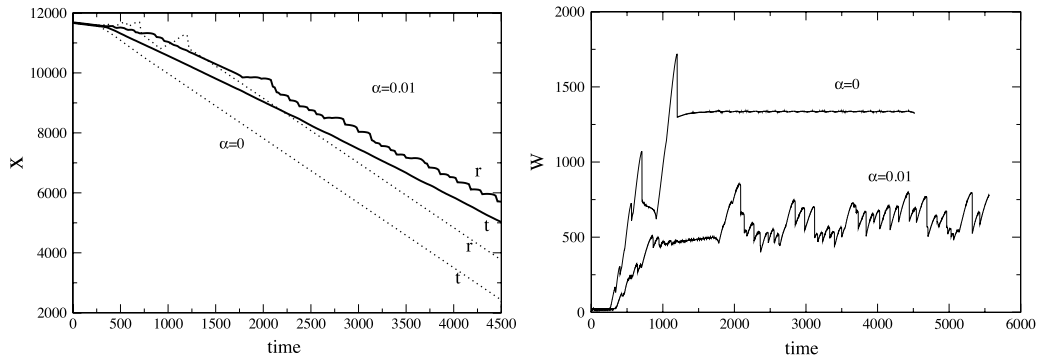


Fig. 5. (left) Temporal evolution of the location of the tip (t) and the rear (r) of the fingering zone for $\alpha = 0$ (dotted lines) and $\alpha = 0.01$ (bold lines) respectively; (right) corresponding mixing length.

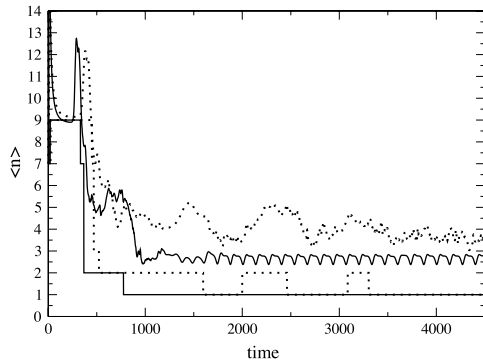


Fig. 6. Power averaged mean wavenumber $\langle n \rangle$ of fingers as a function of time for the conducting ($\alpha = 0.01$, dotted lines) and non conducting ($\alpha = 0$, bold lines) cases. The stepped curves give the temporal evolution of the value of n for the Fourier mode with the largest amplitude.

case considered here. Its typical value is of order -1 as usually $\Delta\rho_c$ and $\Delta\rho_T$ are of the same order [15,26]. As the effect of this parameter has already been studied in detail before [15,26], we keep it to a constant value around $\gamma_T = -3$ typical of a strongly exothermic reaction. The kinetics used in (4) is a simple one-variable cubic scheme known to produce traveling fronts when coupled to diffusion. The kinetic parameter d is here fixed to $d = 0.0021$, a value characteristic of the IAA system [35]. The Damköhler number Da is a dimensionless parameter expressing the ratio between the hydrodynamic and chemical time scales. It is of order 1 for the IAA reaction [35] and takes smaller values close to $Da = 0.001$ [15,41] for the CT reaction. As the effect of the Damköhler number has already been analyzed in details before [22,35,38,41], we will keep it here to typical intermediate values close to 0.1 for which first studies of the influence of heat losses have already been performed [34]. The Lewis number Le

is defined as the ratio between the thermal and solutal diffusion coefficients. Its value ranges between 10 for the CT system [15,34] to larger values around 70 for typical aqueous solutions of small ions. The equation for the temperature (5) further contains a Newton's cooling coefficient α quantifying the intensity of heat losses through the walls. For $\alpha = 0$, the system is insulated and all heat produced by the chemical reaction is kept inside the reactor. For infinite α , all heat immediately escapes through the wall and we effectively analyze an isothermal system. It is difficult to quantify this parameter experimentally, however it is reasonable to take values such that the thermal profile becomes a pulse of given extent rather than a front as is observed experimentally [32]. For the kinetics used here, this is typically achieved with values of α between 0.001 and 0.1 [34]. We are here interested in analyzing nonlinear dynamics for intermediate values of α .

The model thus depends on four parameters, the Damköhler number Da , the Lewis number Le , γ_T the thermal expansion coefficient ruling the density jump due to the heat release during the reaction and α quantifying the heat losses through the walls.

The base state of the problem in the absence of heat losses is a reaction-diffusion (RD) front whereby the stable steady state $(c, T) = (1, 1)$ corresponding to the products invades the unstable one $(c, T) = (0, 0)$ i.e. the reactants. In the absence of convection, the solution of the RD problem is given by [42];

$$c(x, t) = \frac{1}{1 + e^{-\sqrt{Da/2}(x \pm vt)}} \quad (6)$$

where the sign $+$ and $-$ correspond to the ascending and descending front respectively. The reaction front travels with a nondimensional speed $v = \sqrt{Da/2}(1 + 2d)$ and has a width $w = \sqrt{8/Da} \ln[(1 - \delta)/\delta]$, defined as the distance between $c = \delta$ and $c = (1 - \delta)$. In the presence of heat losses (i.e. $\alpha \neq 0$) the base state is not a front but a pulse as the heat produced during the reaction is lost through the walls [34].

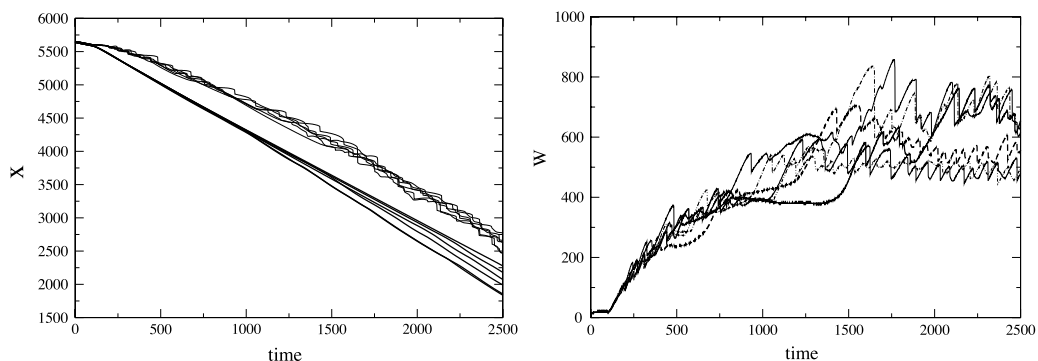


Fig. 7. (left) Location of the tip and rear of the fingering zone and (b) corresponding mixing length as a function of time for six different initial conditions for $Le = 3$, $Da = 0.5$ and $\alpha = 0.01$.

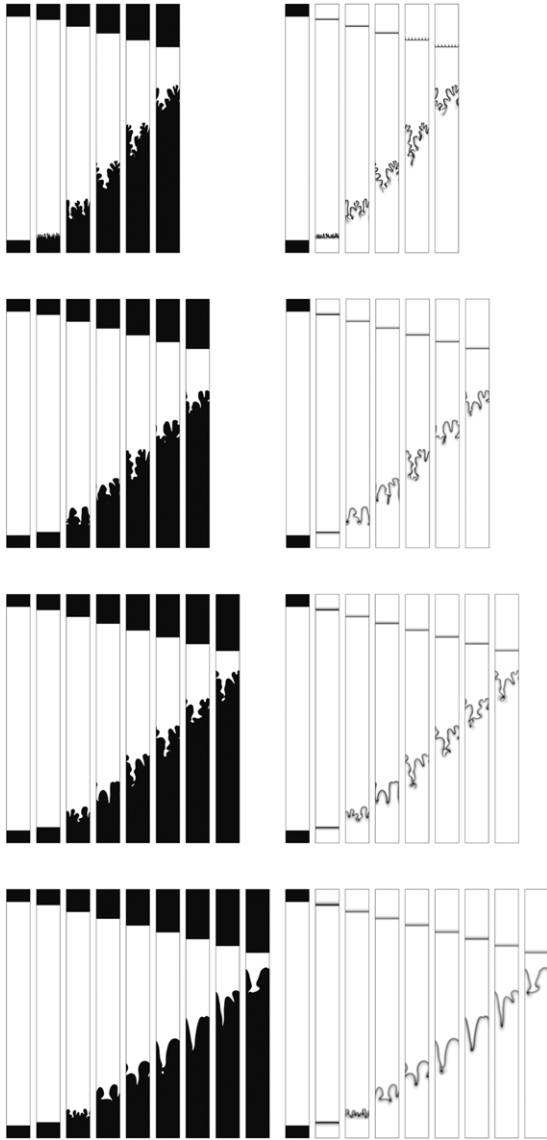


Fig. 8. Nonlinear fingering dynamics of c (left) and T (right) for conducting walls ($\alpha = 0.01$) and four different values of the Lewis numbers $Le = 1, 3, 5$ and 10 (from top to bottom) with $L_y = 768, Da = 0.1, \gamma_T = -3$. From left to right the system is shown at respectively $t = 0$ (i.e. the initial condition) then at every $\Delta t = 500$ up to the time when the two fronts are close to meet.

The density $\rho = (1 - c) + \gamma_T T$ is decreasing during the reaction from $\rho_r = 1$ in the reactants to $\rho_p = \gamma_T$ (with $\gamma_T < 0$) in the products. This induces the fact that upward propagating fronts are unstable as $\rho_p < \rho_r$. Eqs. (1)–(5) are integrated numerically on a spatial domain of length L_x and width L_y using a pseudo spectral method developed by Tan and Homsy [43] and modified to take the chemistry into account [22,34]. We use $dx = dy = 4$ when $Da = 0.1$ and $dx = dy = 2$ when $Da = 0.3$ or 0.5 , the time step is $dt = 0.1$. We have tested that our nonlinear simulations correctly reproduce the predictions of the linear stability analysis [34]. The boundary conditions are periodic in both directions. The reaction is initiated at the same time at both the top and the bottom of the reactor allowing us to follow simultaneously the dynamics of both the downward and upward propagating fronts. Specifically, the initial condition consists in two step functions switching from $c = 1$ to $c = 0$ through one intermediary line where $c = 0.5(1 + 0.001r)$ with r being a random number between 0 and 1. The two steps are located at the axial position x_1 and x_2 respectively sufficiently far apart in both directions along x so that the fluid

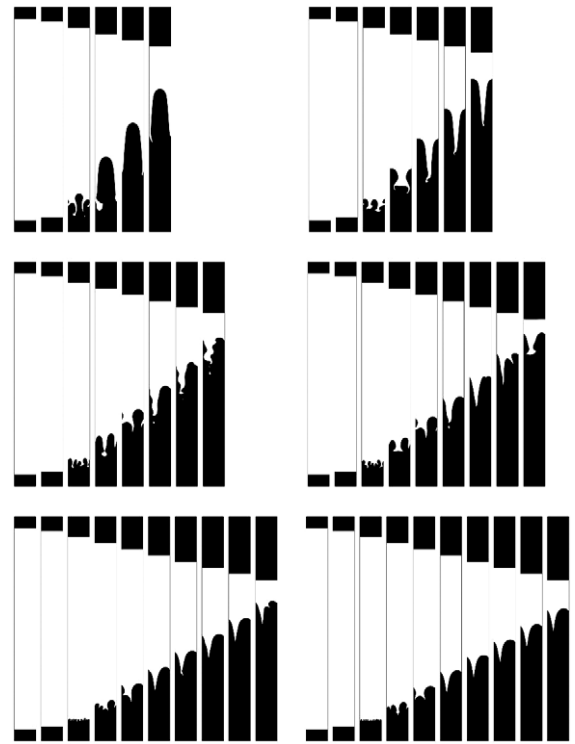


Fig. 9. Nonlinear fingering dynamics of the concentration c for six different values of the cooling coefficient $\alpha = 0, 0.001, 0.005, 0.01, 0.05$ and 0.1 (from left to right and top to bottom). The other parameters are $L_y = 768, Le = 10, Da = 0.1$ and $\gamma_T = -3$. On one figure, the various panels from left to right show the system at respectively $t = 0$ (i.e. the initial condition) then every $\Delta t = 500$ up to the time when the two fronts are close to meet.

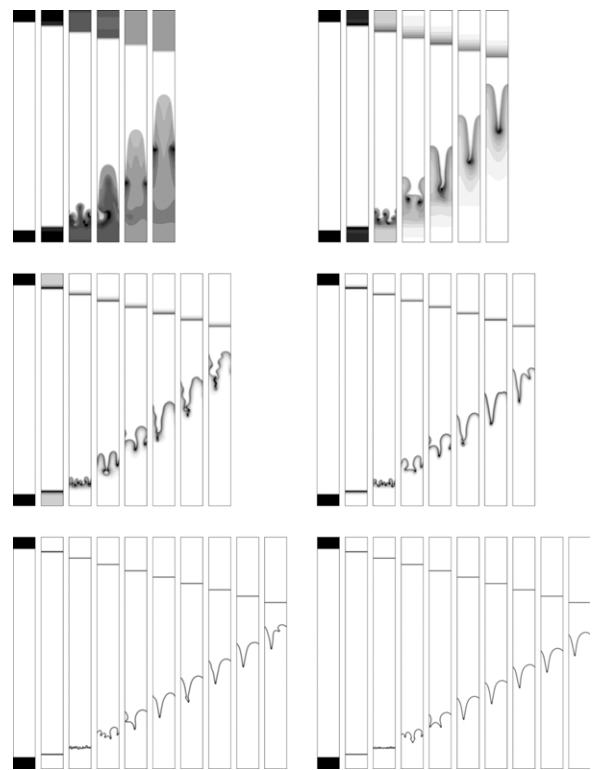


Fig. 10. Same as Fig. 9 but for the temperature.

flow on each front does not interact when fingering sets in. The concentration c is plotted in a scale of grey ranging from $c = 0$

(white) to $c = 1$ (black). The temperature profile on the other hand is plotted in a gray scale ranging from white when $T = 0$ to black, for its maximum value which may be larger than one in the absence of heat losses or smaller than one when heat is dissipated through the walls.

2. Nonlinear dynamics with and without heat losses

We first show two typical non linear dynamics illustrating the main differences between the spatio-temporal evolution of c and T depending whether the system is insulated or not (Fig. 1).

In the case of insulating walls ($\alpha = 0$), we obtain a stable descending front while, for the upward moving front, a rapid merging and coarsening of the fingers leads eventually to one single finger traveling with a constant shape and speed (Fig. 1 top). This trend is logically similar to the one observed numerically for isothermal IAA ascending fronts [21,22]. Indeed, if $\alpha = 0$, the concentration and temperature front profiles both lead to a homogeneous decrease in density across the front. For the small value of Le excluding here differential diffusive effects [23], the descending front features thus a stable stratification of solute light and hot products above solute heavier reactants at room temperature. On the contrary, the ascending front is buoyantly unstable as the heavier and colder reactant solution is now on top. We further note in Fig. 1 for $\alpha = 0$ the presence of hot spots in the valley of the finger where the temperature T is measured to be larger than one i.e. larger than the adiabatic temperature. This temperature excess has been checked to be intrinsic to the reaction-diffusion-convection dynamics as it is robust towards numerical mesh and time-step refinements. In addition, the presence of such hot spots has been evidenced experimentally recently in the case of the chlorite-tetrathionate reaction and results from an increased transport of fresh reactants by advection towards the valleys of the fingers [32].

For conducting walls i.e when $\alpha \neq 0$ we see that, as predicted theoretically [34], the downward propagating front is unstable due to a locally unstable stratification of cooled products behind the front above hotter products inside the front. The cellular deformation of the front features frozen fingers of a small and constant amplitude and fixed wavelength (Fig. 1 bottom). The instability remains confined inside the temperature pulse because of the presence below the front of a stable region where the products heated inside the front lie above the cool reactants. This is coherent with the fact that the corresponding dispersion curves witness a fixed band of unstable modes with the long wave modes being stable [34]. This has already been shown previously to freeze the pattern and inhibit coarsening [15]. For the upward propagating front, the asymptotic dynamics of the finger is totally different with the heat losses through the walls leading to enhanced tip splitting.

Seeing that thermal effects have a drastically different influence on the dynamics depending whether the system is insulated or not, our goal is here to compare quantitatively the fingering characteristics in the presence of thermal effects (with and without heat losses) to the isothermal case presented in [22]. This comparison can be made thanks to various types of measurements [22] that we now explain.

2.1. Averaged profiles

During the course of time, the two-dimensional concentration field $c(x, y, t)$ can be spatially averaged along either the x or y coordinate yielding one-dimensional averaged profiles. The transversely averaged profile is defined as

$$\langle c(x, t) \rangle = \frac{1}{L_y} \int_0^{L_y} c(x, y, t) dy \quad (7)$$

and is shown on Fig. 2 for the nonlinear simulations of Fig. 1.

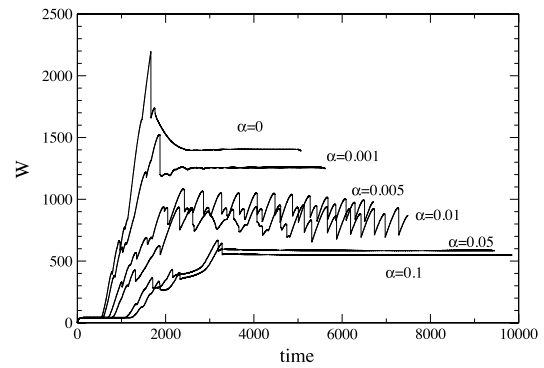


Fig. 11. Mixing length as a function of time for different values of α . The other parameters are $L_y = 512$, $Le = 5$, $Da = 0.1$ and $\gamma_T = -3$.

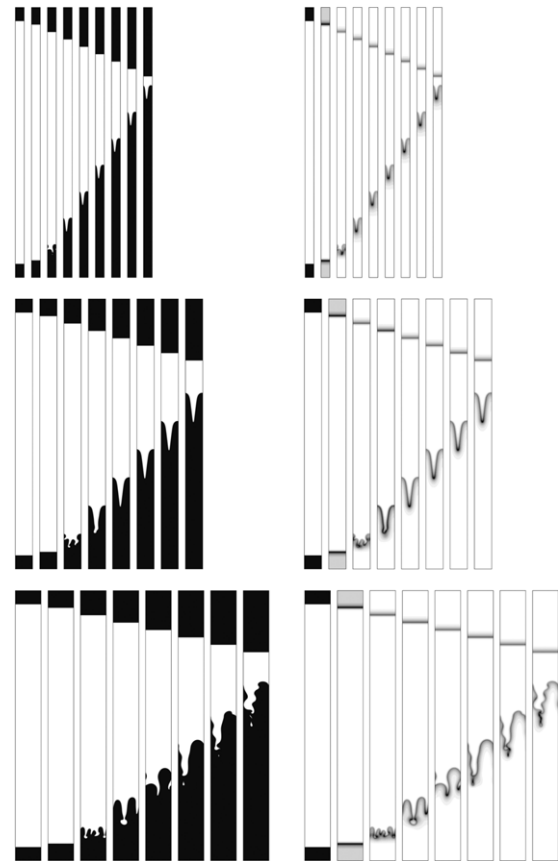


Fig. 12. Nonlinear fingering dynamics of c and T for different widths $L_y = 256$, 512 and 768 (from top to bottom) with $\alpha = 0.005$, $Le = 10$, $Da = 0.1$ and $\gamma_T = -3$. From left to right the system is shown at respectively $t = 0$ (i.e. the initial condition) then every $\Delta t = 500$ up to the time when the two fronts are close to meet.

If the traveling front is stable, as for the descending front at $\alpha = 0$, we recover in this profile, the hyperbolic tangent front solution (6) for c and the corresponding traveling temperature front. On the contrary, as soon as fingering starts as for the ascending front, bumps appear in $\langle c(x, t) \rangle$ as can be seen in Fig. 2 at large x . The asymptotic single finger reached eventually when $\alpha = 0$ appears in these transversely averaged profiles as a deformed traveling front moving with a constant shape and speed as for isothermal systems [22]. In the corresponding 1D averaged temperature profile, the presence of the hot spot seen in Fig. 1 is witnessed by the fact that the maximum value of $\langle T(x, t) \rangle$ is larger than one.

The presence of heat losses modifies these various properties. For the downward moving fronts, the small amplitude fingering is

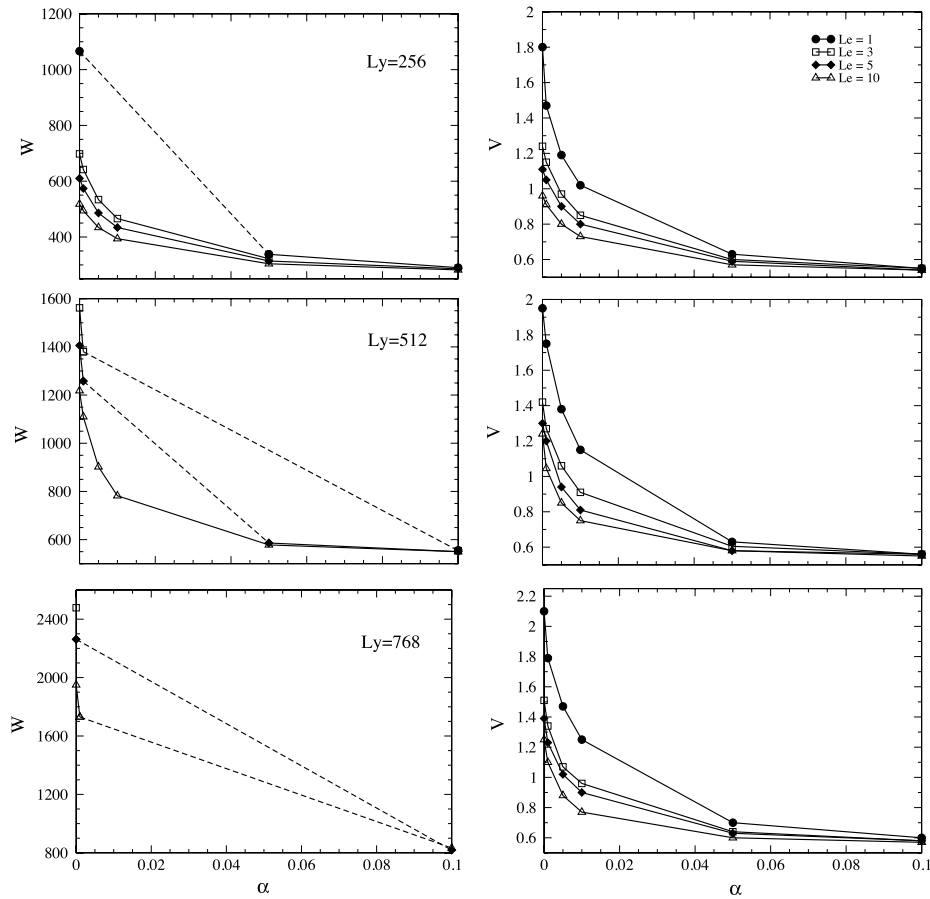


Fig. 13. Asymptotic value of the mixing length W and of the propagation speed V as a function of α for three different widths $L_y = 256, 512$ and 768 from top to bottom, four different Lewis numbers $Le = 1, 3, 5$ and 10 and six different values of $\alpha = 0, 0.001, 0.005, 0.01, 0.05, 0.1$. The other parameters are set to $Da = 0.1, \gamma_T = -3$. For all values represented by the dashed line, the system has not saturated to one single finger but undergoes repetitive tip splitting.

too weak to be seen on the transverse profiles, however the switch in the temperature profiles from fronts to pulses is clearly obtained when α is non zero any longer. The maximum temperature value is lower than one and decreases once convection sets in. For the upward moving front, the averaged profiles are strongly deformed by convection. The succession of tip splitting events is such that no constant deformation is reached, but an irregular succession of bumps remains in the course of time both in the concentration and temperature 1D transversely averaged profiles (Fig. 2 right column). Moreover, convection spreads out the heat as we observe a lower amplitude of the thermal pulse when the front is strongly buoyantly unstable.

The longitudinally averaged profiles defined as

$$\langle c(y, t) \rangle = \frac{2}{L_x} \int_0^{L_x/2} c(x, y, t) dx \quad (8)$$

illustrate on the other hand how fingers on an ascending front can interact, spread and shield their neighbors or merge to ultimately lead to one asymptotic single finger (see Fig. 3 for $\alpha = 0$) or to a finger featuring tip splitting (Fig. 3 for $\alpha = 0.01$). An analogous definition is obtained for the descending front where now the integral runs from $L_x/2$ to L_x . In the same Fig. 3, we see that the downward propagating front features on such profiles a weak deformation and a constant wavelength when heat losses are able to destabilize it.

A good way to appreciate the changes in the wavelength of the dynamics independently of the amplitude of the cellular deformation is to plot a space–time diagram of the locations of the maxima and minima of the transverse averaged profile $\langle c(y, t) \rangle$

in the course of time (see Fig. 4) [44]. Such a diagram shows the mechanism of shielding of fingers by their spreading neighbor and the subsequent reordering of the positions of the extrema until the remaining of one ultimate single finger for the ascending front in an insulated reactor. For conducting walls, it allows us to appreciate the constant wavelength character of the downward moving front modulation and the strongly irregular dynamics due to splittings of the ascending ones.

2.2. Tip, rear and mixing length of the fingered zone

The transversely averaged profile is next used to define the tip and rear of the fingered zone as the location along the x axis for which $\langle c(x, t) \rangle$ is respectively smaller than 0.01 and larger than 0.99. These points correspond respectively to the most and less advanced locations of the fingered zone. Fig. 5 shows the temporal evolution of the position of the tip and rear for the two ascending fronts of Fig. 1. Starting from a step function as initial condition, the planar reaction-diffusion front establishes first in which tip and rear move in parallel separated by a fixed distance w at the same speed v . This reaction-diffusion dynamics is only present at the beginning. After a given induction time, fingering sets in and the tip starts to move at a still constant but larger nonlinear speed V resulting from the nonlinear interaction between the convection rolls and the traveling front. The rear of the front is entrained by the chemical front. The observed bumps correspond to disappearances of the tail of white ($c = 0$) fingers in the black ($c = 1$) background as the traveling front is moving up. For insulated systems, after all fingers have merged and only one single finger remains, the rear

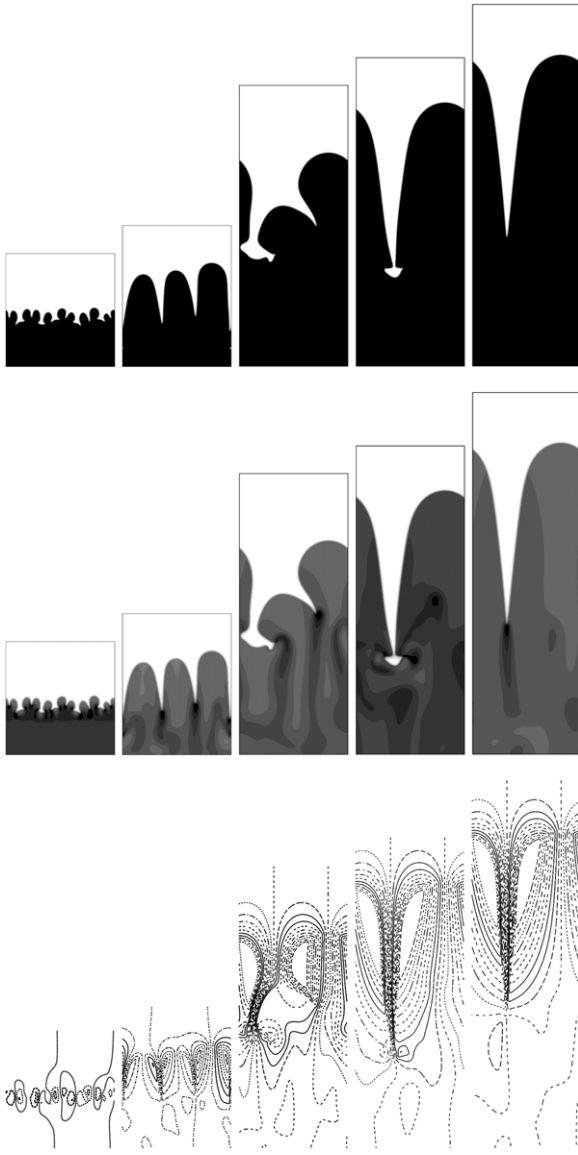


Fig. 14. Concentration c , temperature T and streamlines from top to bottom for the insulated case $\alpha = 0$ and $Le = 3$, $Da = 0.5$, $\gamma_T = -3$. On one line, the snapshots show the dynamics at successive times $t = 200, 600, 1000, 1400$ and 1800 . In the final single finger limit, the velocity field features two counter-rotating vortices.

travels in parallel again with the tip at the nonlinear speed V . The mixing length L , defined as the distance between the tip and the rear, reaches then a constant value W larger than the reaction-diffusion width w of the stable planar front. When $\alpha \neq 0$, the tip still travels at a constant speed but the rear position repetitively varies depending on the splitting events giving rise to a mixing length L changing irregularly in time. Let us note that fingering shows a shorter induction time and a higher slope of the initial linear growth of the mixing length for $\alpha = 0$ compared to the case when heat is dissipated through the walls. This is coherent with the linear stability analysis results that show that the system is more unstable for isolated systems in the case of ascending cooperative fronts [34].

2.3. Power averaged mean wavenumber

In absence of tip splittings, the nonlinear dynamics of the system is dominated by coarsening of the fingers [22]. A convenient quantitative measure of this phenomenon is provided by the

power averaged mean wavenumber defined as

$$\langle k(t) \rangle = \frac{\sum_i k_i P_i}{\sum_i P_i} \quad (9)$$

where k_i are the Fourier modes of the Fourier transform $\hat{c}(k, t)$ of the transversely averaged profile $\langle c(y, t) \rangle$ and $P(k) = |\hat{c}(k)|^2$ their amplitude in Fourier space. The averaged wavelength of the fingers is then simply $\langle \lambda(t) \rangle = 2\pi / \langle k(t) \rangle$ and the power averaged mean number of fingers in the system is then defined as $\langle n \rangle = L_y / \langle \lambda(t) \rangle$.

Fig. 6 shows the temporal evolution of $\langle n \rangle$ as well as of the discrete value of n corresponding to the mode of largest amplitude for the simulations of Fig. 1. These values decrease in time as a consequence of coarsening. In the absence of heat losses, the most unstable mode evolves from 9 fingers initially in the width of the system to 2 and eventually only one single finger as in isothermal systems [22]. The power averaged mean number of fingers $\langle n \rangle$ on the other hand oscillates around the value of 2, the oscillation being related to the oscillatory motion of the minimum seen in the space-time map of Fig. 4 (left). When heat is evacuated through the walls, even though the most unstable mode is also eventually equal to 2, $\langle n \rangle$ evolves erratically because of the succession of tip splitting and merging events.

It is now clear that heat losses influence both qualitatively and quantitatively the properties of fingering of exothermic fronts. Let us now analyze the different trends that arise when varying the thermal parameters Le and α as well as the nondimensional width of the system L_y .

3. Parametric study

Before varying parameters, let us mention that the noise seeding the initial condition is important for the specific dynamics of fingering when tip splitting exists while it is not so important when coarsening towards one single finger is observed. The random noise seeding the initial conditions affects indeed the transient towards the single finger but not its asymptotic properties. However, in presence of tip splittings, the succession of events remain different for each specific initial condition as can be seen on Fig. 7 where six different realizations of the same simulations have been performed changing not the amplitude but the initial spatial distribution of the noise.

As the influence of the Da and γ_T parameters has already been analyzed previously [15,22,26,35,38,41], we keep them constant in this section to the values $Da = 0.1$ and $\gamma_T = -3$. We first vary the Lewis number Le , then study the impact of the heat losses via the parameter α and eventually we focus on the effect of the width of the system L_y .

3.1. Role of Le

Fig. 8 compares the dynamics for values of the Lewis number $Le = 1, 3, 5$ and 10 for $\alpha = 0.01$ and $L_y = 768$. For $Le = 1$ the front propagating upwards features strong tip splitting while the one propagating downwards shows only a weak deformation. When Le is increased, splitting events occur less often but are nevertheless still present even when $Le = 10$. Fig. 8 also shows that the propagation speed is a decreasing function of Le , indeed the front can propagate on longer time scales for increasing Le before meeting the downward propagating front.

3.2. Role of α

We now turn to the impact of α quantifying the intensity of heat losses. The concentration and temperature fields are shown respectively in Figs. 9 and 10 for $Le = 10$ and $L_y = 768$ for six

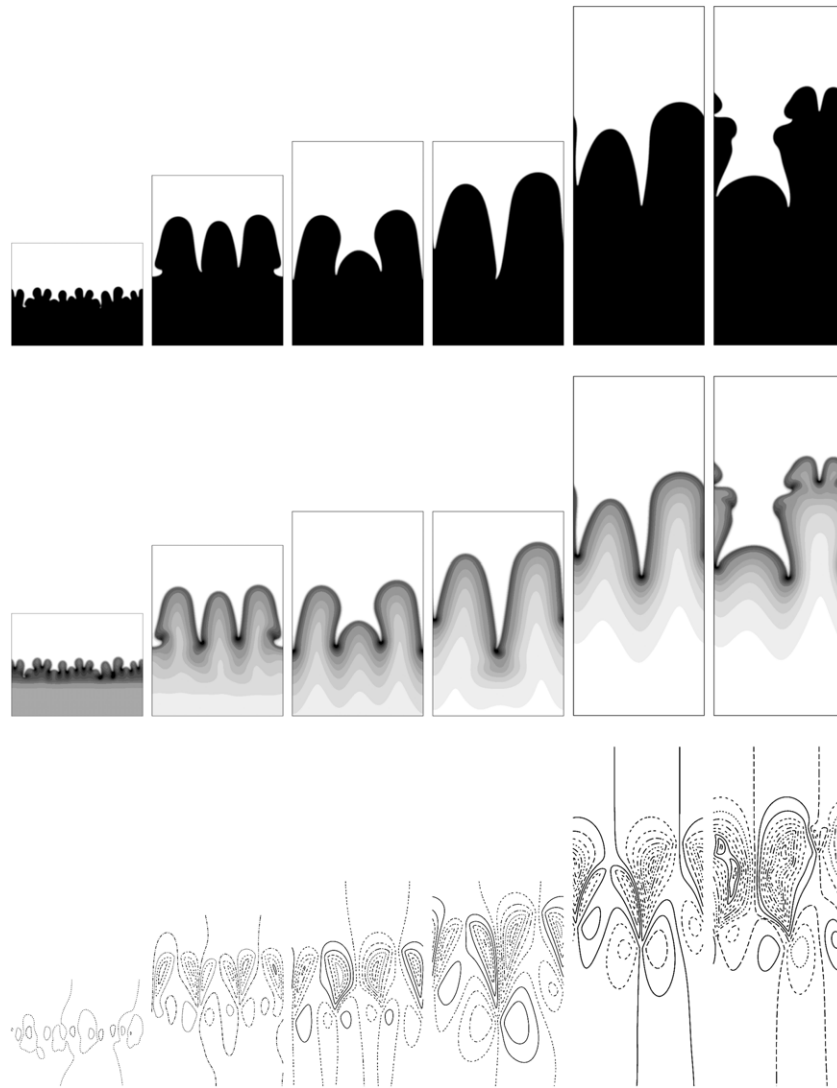


Fig. 15. Similar as in Fig. 14 for conducting walls with $\alpha = 0.005$. On one line, the snapshots show the dynamics at successive times $t = 200, 600, 1000, 1400, 1800$ and 2200 . The velocity field is here characterized by four vortices within each finger.

different α . First of all, increasing α decreases the growth rate as the pattern appears later. This is coherent with the linear stability analysis results [34]. In the nonlinear regime, we see that splitting occurs only for intermediate values of α . If α is too small or too large, the dynamics asymptotes to one single finger the extent of which is longer for $\alpha = 0$ as the total density jump is then larger than for $\alpha = 0.1$ which is closer to the isothermal case. In Fig. 10 we present the corresponding T profiles. Increasing α leads there to more and more heat losses through the walls so that finally only a very thin black stripe of heat is observed around the front when $\alpha = 0.1$. The corresponding dynamics for such large α 's is then in effect the same as the one for an isothermal system [22]. The corresponding mixing length converges hence to a constant for both small or large values of α while it changes erratically in time when splitting events are observed for intermediate values of α (see Fig. 11).

3.3. Role of L_y

The role of L_y is shown in Fig. 12 where three different widths of the system are considered. Larger systems lead to a faster propagating front and to tip splitting while only one single finger is obtained for smaller widths. This is coherent with the nonlinear

dynamics in the isothermal case where larger systems only are shown to exhibit tip splitting [22]. The difference is here that, due to the heat losses through the walls, narrower systems are sufficient to observe tip splitting.

All these effects are summarized in Fig. 13 where the asymptotic value W of the mixing length and the non linear propagation speed V are plotted as a function of α for different values of Le . As already mentioned, even in the presence of tip splitting, it is always possible to extract a propagation speed although this one will slightly vary depending on the initial condition of the simulation. An asymptotic value of the mixing length in the presence of tip splitting is on the other hand difficult to define (see Fig. 7). The graphs of the mixing length in Fig. 13 thus present no quantitative value of W for the values of α leading to tip splitting. We see that increasing L_y leads to more intense splitting, while increasing Le makes the finger less prone to split. For $L_y = 256$ splitting only occurs when $Le = 1$ while for $L_y = 768$, fingers split for nearly all parameter values. Fig. 13 shows moreover that increasing α and Le tends to give fingers of constant length and propagation speed, which of course depend on L_y . These asymptotic values, when compared with the ones obtained for the isothermal case [22], are seen to be a bit larger showing that although the heat effects are very weak for great α they still have some importance.

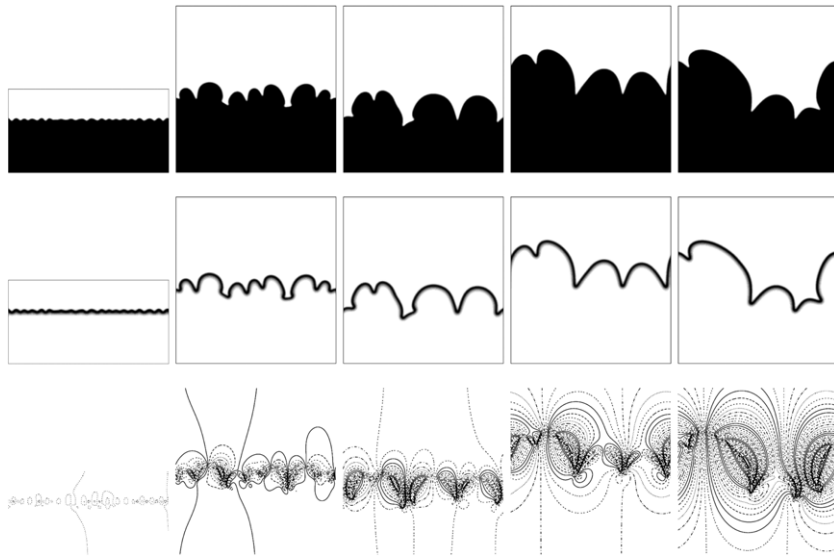


Fig. 16. Similar as in Fig. 14 for conducting walls with $\alpha = 0.1$.

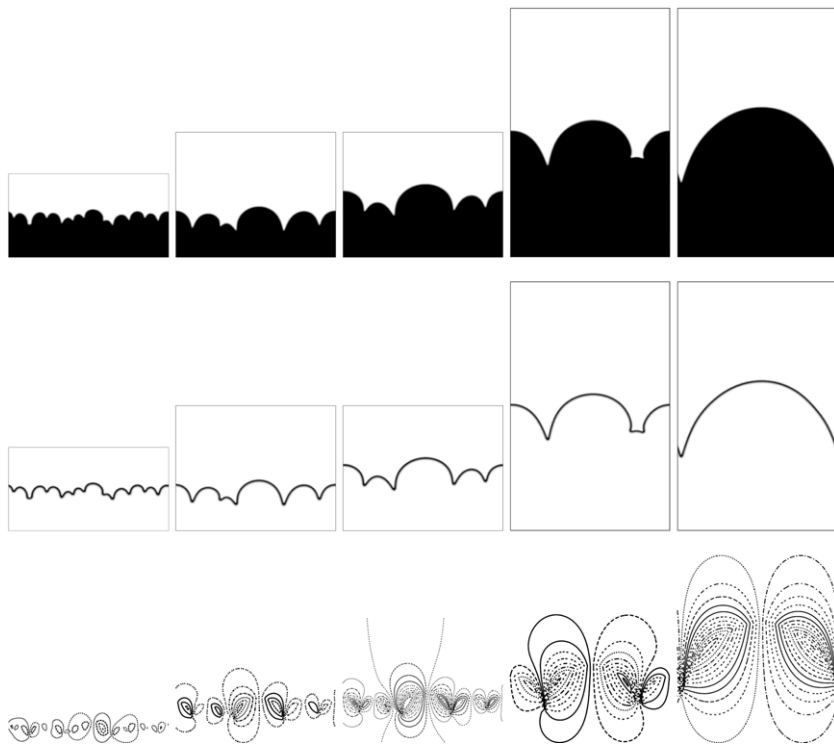


Fig. 17. Similar as in Fig. 14 for conducting walls with $\alpha = 0.5$. On one line, the snapshots show the dynamics at $t = 600, 1000, 1400, 1800$ and finally $t = 4000$.

Let us now focus on the evolution of the flow field during the fingering phenomena enlightening the differences between the conducting and non conducting wall cases.

4. Properties of the fluid flow

In the absence of thermal leaks i.e. for $\alpha = 0$ and cooperative reactions, the nonlinear dynamics has been shown to lead as for isothermal systems [22] to one single finger inside which the velocity field is organized around two counter-rotating vortices as shown in Fig. 14.

The situation is quite different in the case of conductive walls shown in Fig. 15. Here, all parameters are the same as in Fig. 14 except that now $\alpha = 0.005$. First of all, the coarsening trend is

slower and two large fingers are maintained at a later time before the most advanced one starts to split. The temperature profile is not a front anymore but a pulse surrounding the concentration front. As the simulations begin with a step function and as $\alpha = 0.005$ is pretty weak, we see in the two first snapshots that the heat is not completely dissipated yet behind the front. However, quite rapidly when the temperature is larger only in the vicinity of the front, the velocity field features a structure containing four rolls with two counter-propagating vortices behind the front. The origin of this quadrupole of vortices is related to the fact that, across the front, the change of the temperature from $T = 0$ to a positive T inside the front and then back to $T = 0$ far behind the front generates two changes in the sign of the spatial derivative of T , yielding two additional convection rolls [12].

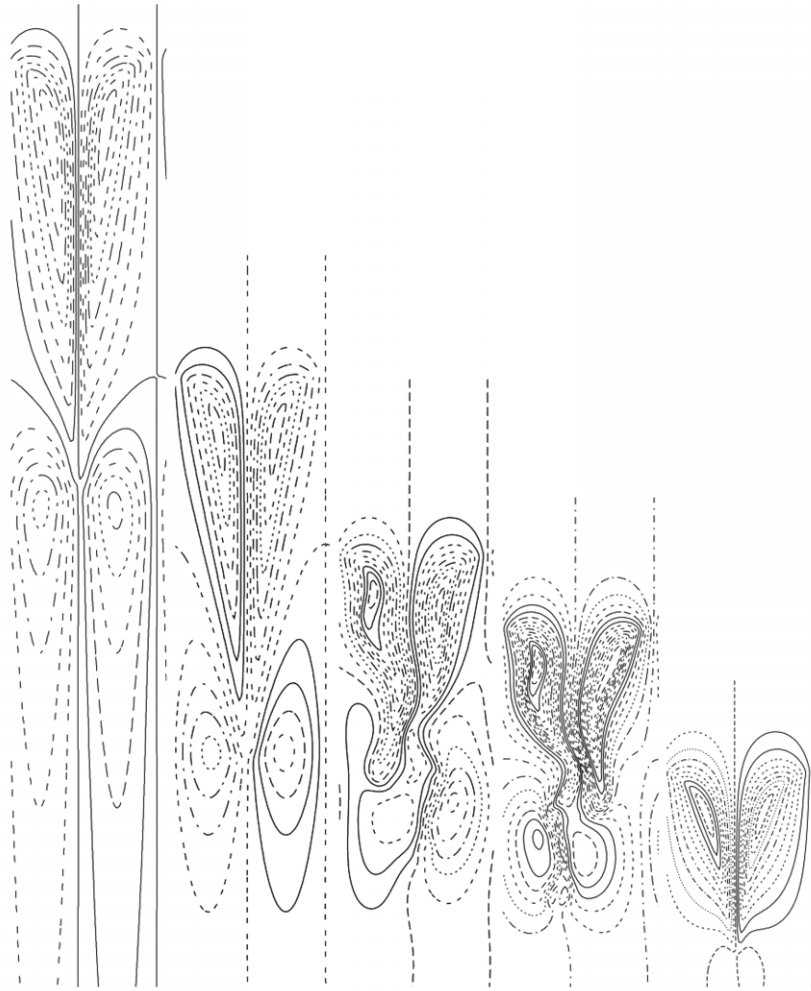


Fig. 18. Streamlines for the insulated and conducting cases for $\alpha = 0, 0.001, 0.005, 0.01$ and 0.05 from left to right and $L_y = 512, Le = 5, Da = 0.1, \gamma_T = -3$ shown at $t = 7000$. The corresponding mixing lengths are given in Fig. 11.

When α is increased in Figs. 15–17 from 0.005 to 0.5, we see a progressive decrease of the longitudinal extent of the flow and of the intensity of convection in the sense that, to represent the isolines we have progressively changed the step between two isoline values from 20 to 5 and then 2. Although the convection strength is getting weaker, splitting phenomena are still present with $\alpha = 0.1$ (Fig. 16). When $\alpha = 0.5$ however, we recover one single finger and two vortices only as most of the heat has now escaped and the system behaves as an isothermal one (Fig. 17). Comparing Figs. 14 and 17, we see that the finger has a smaller extent for large α than for $\alpha = 0$. This is due to the fact that for such cooperative fronts, the total density jump ($\Delta\rho = \Delta\rho_c + \Delta\rho_T$) is larger for $\alpha = 0$ than for large α where in practice $\Delta\rho \sim \Delta\rho_c$.

Eventually, let us mention that we have found in our parametric study that, insulated systems do not always lead to a bipole flow structure but can, in the presence of hot spots for which the temperature locally exceeds one, also feature four vortices. This is the case for the first panel of Fig. 18 obtained for $Le = 5, Da = 0.1, \gamma_T = -3, L_y = 512$ and $\alpha = 0$. The local presence of the hot spot leads to two changes in the derivative of the temperature across the front, which is responsible, as for temperature pulses due to heat losses, to a quadrupole flow structure.

When α is varied successively from $\alpha = 0$ to $\alpha = 0.001, 0.005, 0.01$ and finally $\alpha = 0.05$, tip splitting occurs only for the intermediate values when the four vortices are squeezed one against the other. Four elongated vortices maintained apart for

$\alpha = 0$ or only two convection rolls when heat has escaped from the system for $\alpha = 0.05$ both give one single finger without splitting. It seems thus that the important mechanism for splitting is the squeezing of the two upper convection rolls and not the convection strength.

5. Discussion and perspectives

The nonlinear fingering dynamics of an exothermic traveling chemical front has been studied here numerically in order to quantify the importance of heat losses through the walls of the reactor on the occurrence of tip splitting and characteristics of the velocity field. We have focused on the case of cooperative fronts for which the thermal and solutal density contributions to the total density jump across the front have the same sign and both decrease the density during the reaction. We have in particular made a parametric study of the influence on the dynamics of the intensity of heat losses through the walls, of the Lewis number and of the width of the system.

Our analysis emphasizes the marked influence of the heat losses through the plates whereby the temperature profile is no longer a front but a pulse centered around the front. The nonlinear dynamics in the case of insulating walls features coarsening of Rayleigh–Taylor unstable ascending fronts towards one single finger propagating at a speed larger than the reaction-diffusion one just as observed in isothermal systems [21,22]. Hot spots

can then be observed. The situation is dramatically different for conducting walls where we observe destabilization of descending fronts by a small amplitude modulation and enhanced splitting phenomena for ascending fronts. These tip splitting events are observed to occur more frequently for intermediate values of α , the single finger dynamics being recovered for large α 's corresponding in effect to the equivalent of isothermal systems. At fixed intermediate value of α , the asymptotic speed of the fingered zone as well as the number of splitting events both decrease when Le increases as the thermal field is then more spread out.

We have furthermore studied the properties of the flow field evolution for various values of the heat loss rate α . The properties of the flow field are different whether the walls are insulating or conducting. In insulating systems, the flow field inside one finger features only one pair of vortices but can in some cases show four vortices if a hot spot is present. A quadrupole of flow vortices arranged around a saddle-node structure is obtained as well in the presence of heat losses of intermediate intensity [32].

Our results demonstrate an increased complexity in the problem when heat losses through the walls are added. We have shown that splitting phenomena can occur for large domains of parameters and that, although the convection strength decreases with increasing α , this strength is not the only factor influencing the splitting phenomena, the structure of the flow field is important as well.

Acknowledgments

This article is dedicated to Professor S.C. Müller. Fruitful discussions with him on the topics of coupling between chemical reactions and hydrodynamic flows are gratefully acknowledged and have been important for our involvement in this research area. A.D. acknowledges financial support of Prodex (Belgium), ESA, FNRS and of the Communauté française de Belgique ("Actions de Recherches Concertées" programme).

References

- [1] H. Miike, S.C. Müller, B. Hess, *Chem. Phys. Lett.* 144 (1988) 515.
 [2] H. Miike, S.C. Müller, B. Hess, *Phys. Rev. Lett.* 61 (1988) 2109.

- [3] H. Miike, S.C. Müller, B. Hess, *Phys. Lett. A* 141 (1989) 25.
 [4] S. Kai, S.C. Müller, T. Mori, M. Miki, *Physica D* 50 (1991) 412.
 [5] H. Miike, H. Yamamoto, S. Kai, S.C. Müller, *Phys. Rev. E* 48 (1993) R1627.
 [6] K. Matthiessen, S.C. Müller, *Phys. Rev. E* 52 (1995) 492.
 [7] M. Diewald, K. Matthiessen, S.C. Müller, H.R. Brand, *Phys. Rev. Lett.* 77 (1996) 4466.
 [8] K. Matthiessen, H. Wilke, S.C. Müller, *Phys. Rev. E* 53 (1996) 6056.
 [9] M. Böckmann, B. Hess, S.C. Müller, *Phys. Rev. E* 53 (1996) 5498.
 [10] M. Böckmann, S.C. Müller, *Phys. Rev. Lett.* 85 (2000) 2506.
 [11] M. Böckmann, S.C. Müller, *Phys. Rev. E* 70 (2004) 046302.
 [12] L. Šebestíková, J. D'Heroncourt, M.J.B. Hauser, S.C. Müller, A. De Wit, *Phys. Rev. E* 75 (2007) 026309.
 [13] I.R. Epstein, J.A. Pojman, *An Introduction to Nonlinear Dynamics: Oscillations, Waves, Patterns and Chaos*, Oxford University Press, New York, 1998.
 [14] J.A. Pojman, I.R. Epstein, *J. Phys. Chem.* 94 (1990) 4966.
 [15] S. Kalliadasis, J. Yang, A. De Wit, *Phys. Fluids* 16 (2004) 1395.
 [16] J. D'Heroncourt, A. Zebib, A. De Wit, *Chaos* 17 (2007) 013109.
 [17] D. Horváth, T. Bánsági Jr., A. Tóth, *J. Chem. Phys.* 117 (2002) 4399.
 [18] T. Bánsági Jr., D. Horváth, Á. Tóth, *Phys. Rev. E* 68 (2003) 026303.
 [19] J.A. Pojman, I.R. Epstein, T.J. McManus, K. Showalter, *J. Phys. Chem.* 95 (1991) 1299.
 [20] J. Masere, D.A. Vasquez, B.F. Edwards, J.W. Wilder, K. Showalter, *J. Phys. Chem.* 98 (1994) 6505.
 [21] J. Huang, B.F. Edwards, *Phys. Rev. E* 54 (1996) 2620.
 [22] A. De Wit, *Phys. Fluids* 16 (2004) 163.
 [23] J. D'Heroncourt, A. Zebib, A. De Wit, *Phys. Rev. Lett.* 96 (2006) 154501.
 [24] J.A. Pojman, I.P. Nagy, I.R. Epstein, *J. Phys. Chem.* 95 (1991) 1306.
 [25] J. D'Heroncourt, A. De Wit, A. Zebib, *J. Fluid Mech.* 576 (2007) 445.
 [26] T. Bánsági Jr., D. Horváth, Á. Tóth, J. Yang, S. Kalliadasis, A. De Wit, *Phys. Rev. E* 68 (2003) 055301.
 [27] T. Bánsági Jr., D. Horváth, Á. Tóth, *Chem. Phys. Lett.* 384 (2004) 153.
 [28] T. Tóth, D. Horváth, Á. Tóth, *Chem. Phys. Lett.* 442 (2007) 289.
 [29] I. Nagypál, G. Bazsa, I.R. Epstein, *J. Am. Chem. Soc.* 108 (1986) 3635.
 [30] I.P. Nagy, J.A. Pojman, *J. Phys. Chem.* 97 (1993) 3443.
 [31] D.A. Bratsun, Y. Shi, K. Eckert, A. De Wit, *Europhys. Lett.* 69 (2005) 746.
 [32] P. Grosfils, C. Yourassowsky, F. Dubois, A. De Wit, *Phys. Rev. E* 79 (2009) 017301.
 [33] L. Rongy, G. Schuszter, Z. Sinkó, T. Tóth, D. Horváth, A. Tóth, A. De Wit, *Chaos* 19 (2009) 023110.
 [34] J. D'Heroncourt, S. Kalliadasis, A. De Wit, *J. Chem. Phys.* 123 (2005) 234503.
 [35] A. De Wit, *Phys. Rev. Lett.* 87 (2001) 054502.
 [36] J. Martin, N. Rakotomalala, D. Salin, M. Böckmann, *Phys. Rev. E* 65 (2002) 051605.
 [37] M.R. Carey, S.W. Morris, P. Kolodner, *Phys. Rev. E* 53 (1996) 6012.
 [38] D. Lima, W. van Saarloos, A. De Wit, *Physica D* 218 (2006) 158.
 [39] T. Bánsági Jr., D. Horváth, Á. Tóth, *J. Chem. Phys.* 121 (2004) 11912.
 [40] T. Rica, D. Horváth, Á. Tóth, *Chem. Phys. Lett.* 408 (2005) 422.
 [41] J. Yang, A. D'Onofrio, S. Kalliadasis, A. De Wit, *J. Chem. Phys.* 117 (2002) 9395.
 [42] A. Saul, K. Showalter, in: R.J. Field, M. Burger (Eds.), *Oscillations and Traveling Waves in Chemical Systems*, Wiley, New York, 1985.
 [43] C.T. Tan, G.M. Homsy, *Phys. Fluids* 31 (1988) 1330.
 [44] J. D'Heroncourt, J.H. Merkin, A. De Wit, *J. Chem. Phys.* 130 (2009) 114503.